*Tetrahedron* Vol. 49, No. 27, pp. 5927-5940, 1993
Printed in Great Britain

0040-4020/93 $6.00+.00


# Crystal Structure, Conformational Analyses, and Charge Density Distributions for *Ent*-Epifisetinidol: an Explanation for Regiospecific Electrophilic Aromatic Substitution of 5-Deoxyflavans

Fred L. Tobiason,[a*] Frank R. Fronczek,[b] Jan P. Steynberg,[c,d]
Elizabeth C. Steynberg,[c,d] and Richard W. Hemingway[c]

[a] *Department of Chemistry, Pacific Lutheran University, Tacoma, WA 98447, U.S.A.*

[b] *Department of Chemistry, Louisiana State University, Baton Rouge, LA 70803, U.S.A.*

[c] *Southern Forest Experiment Station, USDA Forest Service, Pineville, LA 71360, U.S.A.*

(*Received in USA* 23 *April* 1993)

ABSTRACT. — Molecular modeling and molecular orbital analyses of *ent*-epifisetinidol gave good predictions of the approximate "reverse half-chair" conformation found for the crystal structure. MNDO[a] and AM1 analyses of HOMO electron densities provided an explanation for the stereospecific electrophilic aromatic substitution at C(6) in 5-deoxy-flavans.

Most of the commercial and biological significance of condensed tannins lies in their complexation with other bio-polymers (proteins and carbohydrates). Although the condensed tannins have been studied intensively,[1-4] the mechanisms of polyflavanoid complexation with proteins and carbohydrates remain comparatively obscure. In order to explain the interactions of polyflavanoids with other biological polymers such as proteins, it is essential that conformation and complexation properties of polyflavanoids be better understood. For example, these interactions impact animal nutrition,[5] herbivory by insects[6] and ruminant animals,[7,8] as well as practices in the manufacture of leather[9] and even the flavor qualities of various beverages.[10-12]

Key to understanding these interactions is obtaining more knowledge of the conformations (and conformational flexibility) of the polyflavanoids.[4,13] It is unfortunate that so little is known about the conformation of polyflavanoid polymers given their important commercial and ecological roles. Among the monomeric flavan-3-ols, only the crystal structures of (-)-epicatechin[14] and 2R,3S,4R-(+)-3,3',4,4',5,7-penta-*O*-hexahydroxyflavan-dihydrate[15] have been described in the free phenolic form. Derivatives [e.g., tetra-*O*-methyl-(+)-catechin,[16] penta-*O*-acetyl-(+)-catechin,[17] both 6- and 8-bromo-tetra-*O*-methyl-catechin,[18,19] and a permethylated procyanidin-4-phloroglucinol adduct[20]] have been described, but such derivatization distorts the conformation of these compounds.[17] Therefore, the crystal structures of these methylated or acetylated derivatives are of limited application in the understanding of the natural polymers.

[d]Work performed while visiting scientists at the Southern Forest Experiment Station, USDA Forest Service, Pineville, LA, from the Department of Chemistry, University of the Orange Free State, Bloemfontein, South Africa.

[e]Reference to commercial trade names does not imply endorsement by the U.S. Department of Agriculture.

Mattice and coworkers[21] have studied the conformations of procyanidins and prodelphinidins through application of molecular mechanics and study of their fluorescence spectra.[22] More recently, Steynberg and coworkers[23] have extended these analyses to the C(5)-deoxy profisetinidins (the most important polyflavanoids of commerce), wattle and quebracho tannins.

To obtain more physical data for studies of the structure of the 3,7,3',4'-tetrahydroxy flavans (profisetinidins), the crystal structure of *ent*-epifisetinidol [1] (Figure 1) was studied. These data were compared to those obtained previously for (-)-epicatechin [2]. The crystal structure data for *ent*-epifisetinidol were then compared with conformational properties predicted from molecular mechanics [Alchemy-II, MMIIPC, MMX, and MMP2(87) force fields] and semi-empirical molecular orbital computations (AM1, MNDO). The comparison of different force fields was made to establish how closely inexpensive PC-based software would match the crystal structure and more elaborate molecular orbital results because many laboratories working with polyflavanoids have access only to PCs. Similar conformational analyses have been made for (-)-epicatechin.[14,23,24]

In addition to comparing conformations predicted by different force fields, the interactions governing interrelated rotations of the aliphatic hydroxyl and the B-ring as well as predicting differences in energy barriers to interconversion and differences in total steric energy in the E- and A- conformations for 2,3-*cis* and 2,3-*trans* isomers were of special interest. *Ent*-epifisetinidol and (-)-epicatechin provide excellent models for developing more understanding of the large effect of the C(5)-hydroxyl in reactivity at the C(6) and C(8) positions of polyflavanoids, thus AM1 molecular orbital computations were employed to examine charge density distributions in the A-rings of these compounds.

**Crystal Structure**

*Ent*-epifisetinidol crystallizes as the monohydrate from water as pale tan prisms; monoclinic space group $P2_1$, a = 478.20(4), b = 1154.33(14), c = 1206.43(12) pm; $\beta$ = 93.282(7)°; Dc = 1.460 g cm$^{-3}$; Z = 2, T = 23 °C, R = 0.034 for 2,686 observations (Table 1). The structure [1] was consistent with $^1$H- and $^{13}$C NMR spectral data, and the absolute stereochemistry was verified by optical rotation $[\alpha]_D$ = +76.4° (Figure 1).[25]

Selected bond lengths and torsional angles are summarized and compared with those obtained previously for (-)-epicatechin[14] in Figure 2 and Table 2, respectively. Differences in the bond lengths between *ent*-epifisetinidol and

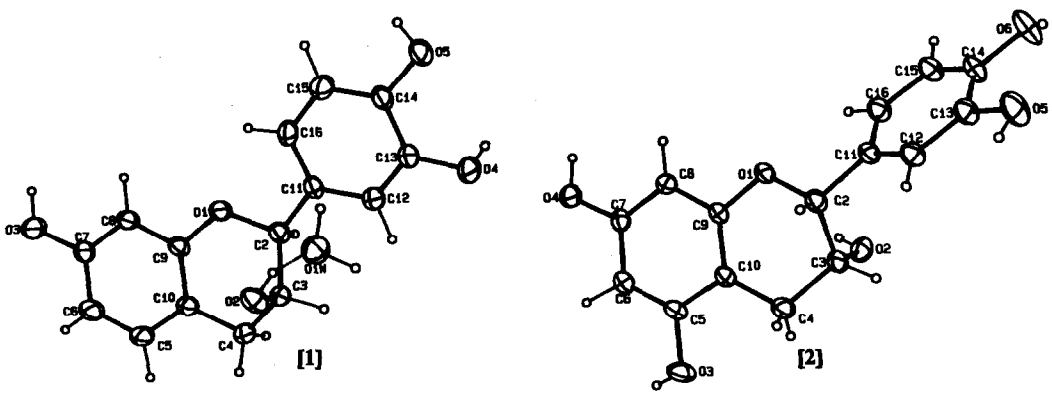


**Figure 1. Crystal structure of *ent*-epifisetinidol as the monohydrate [1] and anhydrous (-)-epicatechin [2].[14]**

**Table 1.** Coordinates for ent-epifisetinidol monohydrate.

| Atom | x | y | z | $B_{eq}(A^2)$ |
|---|---|---|---|---|
| O1 | 0.7253(2) | 0 | 0.07511(5) | 2.96(1) |
| O2 | 0.7529(2) | 0.22864(6) | 0.17584(6) | 2.95(1) |
| O3 | 1.1638(2) | -0.04644(7) | -0.26429(6) | 3.71(1) |
| O4 | 0.2313(2) | 0.03818(8) | 0.51915(6) | 4.16(2) |
| O5 | 0.5997(2) | -0.13949(7) | 0.57112(6) | 3.22(1) |
| C2 | 0.5027(2) | 0.04794(7) | 0.13474(7) | 2.16(1) |
| C3 | 0.4980(2) | 0.18008(7) | 0.12754(7) | 2.23(1) |
| C4 | 0.4645(2) | 0.21693(7) | 0.00647(7) | 2.49(2) |
| C5 | 0.7167(3) | 0.18357(9) | -0.17126(8) | 3.38(2) |
| C6 | 0.8843(3) | 0.11918(9) | -0.23746(8) | 3.73(2) |
| C7 | 0.9957(2) | 0.01488(8) | -0.19726(7) | 2.59(2) |
| C8 | 0.9354(2) | -0.02343(7) | -0.09261(7) | 2.36(2) |
| C9 | 0.7645(2) | 0.04330(7) | -0.02877(6) | 2.08(1) |
| C10 | 0.6521(2) | 0.14818(7) | -0.06550(7) | 2.31(1) |
| C11 | 0.5419(2) | 0.00068(7) | 0.25178(6) | 1.99(1) |
| C12 | 0.3746(2) | 0.04002(8) | 0.33418(8) | 2.69(2) |
| C13 | 0.3983(2) | -0.00485(8) | 0.44122(7) | 2.54(2) |
| C14 | 0.5909(2) | -0.09323(8) | 0.46526(7) | 2.40(2) |
| C15 | 0.7576(3) | -0.13227(9) | 0.38361(9) | 3.25(2) |
| C16 | 0.7361(2) | -0.08517(9) | 0.27748(8) | 2.76(2) |
| O1W | 0.8997(2) | 0.22463(7) | 0.41019(6) | 3.19(1) |

$$B_{eq} = (8\pi^2/3)\Sigma_i\Sigma_j U_{ij} a_i^* a_j^* a_i \cdot a_j$$

(-)-epicatechin are most evident in the heterocyclic ring. Both bonds to the pyran oxygen [C(9)-O(1)-C(2)] are about 1.5 pm shorter and the C(4)-C-(10) bond about 1.1 pm longer in *ent*-epifisetinidol than in (-)-epicatechin. In addition, the C(9)-C(10) and the C(10)-C(5) bonds are about 0.9 and 1.5 pm shorter, respectively, in *ent*-epifisetinidol than in (-)-epicatechin. This implies that there is more $\pi$-bonding to the C(9)-O(1) bond in *ent*-epifisetinidol.

In crystalline *ent*-epifisetinidol, the heterocyclic ring closely approximates a "reverse half-chair" [with only a slight distortion toward a "reverse C(3)-sofa"] in which the B-ring is equatorial [C(9)-O(1)-C(2)-C(11) = -170.00°] and the aliphatic hydroxyl at C(3) is axial [O(1)-C(2)-C(3)-O(2) = -61.46°]. Another way to express the conformation of the heterocyclic ring is through the distances of the C(2) and C(3) atoms from the mean plane of the A-ring (Figure 3). For *ent*-epifisetinidol, the C(2) and C(3) carbons lie 27.83(9) pm below and 40.71(9) pm above the mean plane of the A-ring, respectively. In comparison, the C(2) and C(3) carbons of the (-)-epicatechin crystal[14] lie 26.3 above and 49.5 pm below the mean plane of the A-ring, respectively, with a larger distortion toward a C(3)-sofa conformation.

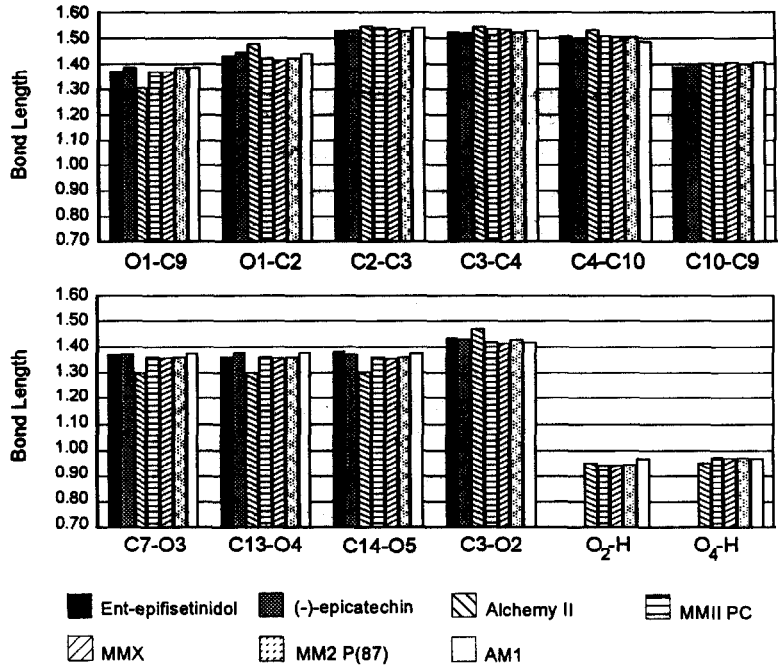


**Figure 2. Comparison of selected bond lengths found for the crystalline monohydrate of *ent*-epifisetinidol, anhydrous crystalline (-)-epicatechin, and estimated for *ent*-epifisetinidol using different modeling methods.**

The C(7)-hydroxyl of the A-ring is closely aligned to the plane of the ring [H-O(3)-C(7)-C(6) = 174.1°] with the hydrogen atom projecting up from the plane of the A-ring by only 9 pm. In contrast to the crystal structure of (-)-epicatechin, the hydroxyls of the catechol B-ring point up away from the aliphatic hydroxyl at C(3) (Table 2). The hydroxyl at C(13) also lies in the plane [H-O(4)-C(13)-C(12) = -177.1°] with the hydrogen atom projecting up from the plane of the B-ring by only 3.6 pm. By contrast, the hydroxyl at C(14) is tipped up away from the plane of the B-ring [H-O(5)-C(14)-C(13) = -157.4°] such that the hydrogen atom projects above the plane 35 pm. Corresponding torsional angles found for (-)-epicatechin in the crystalline state were -160.7° and -167.6°, respectively.

Similar to results found for (-)-epicatechin,[14] the *ent*-epifisetinidol crystal has the hydroxyl at C(3) projecting out away from the pyran ring [H-O(2)-C(3)-C(4) = -169.9° and C(2)-C(3)-O(3)-H = -49.4°]. The other low energy state (see below), in which the C(3) hydroxyl is oriented toward the pyran oxygen, is not found in either crystal. The orientation of the B-ring in *ent*-epifisetinidol [O(1)-C(2)-C(11)-C(12) = 173.6°] differs from that found in (-)-epicatechin [O(1)-C(2)-C(11)-C(12) = 146.6°] in the crystal state.

*Ent*-epifisetinidol molecules and water molecules are involved in the crystal in an intricate network of intermolecular hydrogen bonds. The water molecule is surrounded approximately tetrahedrally by OH groups at distances 2.860(1)--2.939(1)Å, while each OH group engages in two hydrogen bonds, one as donor, and one as acceptor. Angles about H in the six independent hydrogen bonds range 143(2)--164(2)°.

**Table 2.** Selected torsional angles found for the E-conformer of *ent*-epifisetinidol using different molecular modeling force fields compared with the crystal structure of the monohydrate and with an MMX optimized conformation for (-)-epicatechin.

| Torsional | *Ent*-Entifisetinidol Crystal | (-)-Epicatechin (MMX) | Alchemy-II | MMII PC | MMX | MM2P(87) | AM1 |
|---|---|---|---|---|---|---|---|
| **Heterocyclic Ring** | | | | | | | |
| C(8)-C(9)-O(1)-C(2) | -165.4(0.07) | 166.5 | -164.5 | -167.4 | -166.9 | -167.9 | -160.4 |
| C(9)-O(1)-C(2)-C(3) | -45.0(0.10) | 44.2 | -47.6 | -46.2 | -43.1 | -42.7 | -51.1 |
| O(1)-C(2)-C(3)-C(4) | 58.6(0.10) | -59.2 | 60.7 | 62.9 | 58.8 | 60.2 | 60.7 |
| C(2)-C(3)-C(4)-C(10) | -44.5(0.10) | 46.2 | -46.9 | -46.6 | -46.9 | -46.7 | -38.8 |
| O(1)-C(9)-C(10)-C(4) | -3.6(0.14) | -0.2 | 0.0 | 0.1 | -0.7 | 0.8 | 0.2 |
| H(2)-C(2)-C(3)-H(3) | 60.8 | -65.2 | 61.6 | 66.7 | 64.7 | 65.1 | 62.5 |
| **B-ring** | | | | | | | |
| C(9)-O(1)-C(2)-C(11) | -170.0(0.10) | 168.3 | -169.0 | -170.4 | -167.0 | -163.7 | -174.3 |
| H(2)-C(2)-C(11)-C(12) | -69.9 | 30.1 | -53.3 | -38.5 | -31.8 | -38.0 | -36.5 |
| O(1)-C(2)-C(11)-C(12) | 173.6(0.08) | 146.6 | -174.1 | -155.6 | -148.2 | -155.0 | -153.4 |
| **Aliphatic Hydroxyl** | | | | | | | |
| H(3)-C(3)-O(2)-H | 69.1 | -47.9 | 59.9 | 55.4 | 46.5 | 71.1 | 93.0 |
| C(2)-C(3)-O(2)-H | -49.4(1.3) | 72.4 | -61.4 | -65.8 | -73.8 | -48.4 | -27.7 |
| O(1)-C(2)-C(3)-O(2) | -61.5 | 61.8 | -58.4 | -57.4 | -61.6 | -60.6 | -59.5 |
| **Aromatic Hydroxyl** | | | | | | | |
| C(6)-C(7)-O(3)-H* | 174.1(1.5) | -177.7 | 176.9 | 179.0 | 178.9 | 179.1 | 179.4 |
| C(12)-C(13)-O(4)-H* | 177.1(1.9) | -2.5 | -176.1 | 179.4 | 179.2 | -179.7 | 179.4 |
| C(13)-C(14)-O(5)-H* | 157.4(1.1) | -0.7 | 180.0 | 179.3 | 177.9 | -179.0 | 178.6 |

*Oxygen atoms O(4), O(5), and O(6) in (-)-epicatechin.

## Conformational Analyses

In addition to the description of the (-)-epicatechin crystal structure,[14] this compound has been studied intensively by Tobiason[24] using MM2P(87), MM2, MNDO, and AM1, and Steynberg[23] using MM2, MMX, PM3, MNDO, and AM1. These analyses centered primarily on three questions: 1) the conformation of the heterocyclic ring, 2) the interrelated orientations of the catechol B-ring and the aliphatic 3-hydroxyl, and 3) the inter-conversion between A- (axial B-ring) and E- (equatorial B-ring) conformers as well as obtaining estimates of the relative proportions of the two in solution. The latter question has been addressed by $^1$H NMR spectroscopic and molecular modeling methods.

These same questions were addressed here relative to *ent*-epifisetinidol, and the results were compared to those obtained in studies of (-)-epicatechin.[23,24] The Alchemy-II and MMIIPC force fields were also examined in an attempt to determine how well these comparatively inexpensive programs operating on personal computers would compare to the more elaborate molecular mechanics and molecular orbital methods. In the following discussions, the structures modeled were lower in energy than the crystal structure, but not necessarily that of the global minimum energy.

Bond lengths found in the crystal and as obtained from the various molecular modeling methods are summarized in Figure 2. Alchemy-II (a Tripos force field) is especially convenient to use to obtain structural data reasonably close to crystal structure data. However, $C_{Ar}$-O bonds were consistently underestimated by approximately

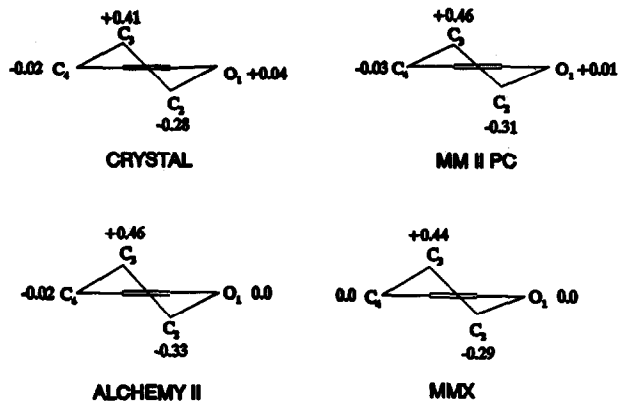


**Figure 3. Heterocyclic ring conformations in the crystal and as predicted by various molecular mechanics force fields.**

7 pm, whereas, $C_{Aliph}$-O bonds lengths were overestimated by approximately 4 pm using the Alchemy-II force field. MMIIPC [accounting for aromatic character of the A- and B-rings by using Allinger MM2 force field constants modified by $\pi$-molecular orbital calculations (Table 3) from MMP2(87) on (+)-catechin and (-)-epicatechin] and MMX (which includes $\pi$-VESCF routines)] gave very similar results. In comparison to the crystal structure for *ent*-epifisetinidol, these methods underestimated $C_{Ar}$-O and $C_{Aliph}$-O bond lengths within the pyran ring by about 5 and 10 pm, respectively. A similar result was found in MM2 and MMX analyses of (-)-epicatechin.[23,24] Bond lengths estimated by AM1 molecular orbital methods give satisfactory agreement with the crystal structure, generally within $\pm$ 1 pm. Where discrepancies exist, most values are slightly larger except for the C(3)-O(2) and C(4)-C(10) bonds, which are about 2 pm shorter. The AM1 calculations show a C(3)-OH effect with the lowest energy conformations given with the H(3)C(3)O(2)H angle being about 168° where the OH is directed into the pyran ring. The higher energy equatorial conformation data given in Table 2 are for the C(3)-OH in the orientation found in the crystal structure. MNDO geometry parameters are never found to fit as well as AM1 determined parameters do.[24]

A summary comparison of selected dihedral angles found in the crystal structure of *ent*-epifisetinidol and as estimated by various modeling methods is given in Table 2. As a further comparison, the conformation of (-)-epicatechin as projected using the MMX force field is presented. As was found in the crystal state, molecular mechanics [Alchemy-II, both MMIIPC and MMX, and MM2P(87)] predicts a "reverse half-chair" with some distortion toward a "reverse C(3)-sofa" conformation for *ent*-epifisetinidol (Figure 3). Considering the torsion angles in Table 2, the Alchemy-II force field most closely predicts the heterocyclic ring conformation found in the crystal state despite the poor correspondence to the crystal structure in terms of bond lengths to the pyran oxygen atom. However, even though MMX (and MM2(87)) seem to distort the pyran ring torsion angles relative to the crystal, they give a respectable out-of-plane distance for C(2), see Figure 3. The AM1 molecular orbital calculations favor a C(2) sofa conformation (Table 2).

**Table 3.** Torsional, bending and stretching MM computational parameters adjusted for MO bond orders currently developed for flavans.

| Torsional Parameters | | | | | | |
|---|---|---|---|---|---|---|
| Atom Type | | | | V1 | V2 | V3 |
| 2 | 2 | 2 | 2 | -0.93 | 4.80 | 0.00 |
| 2 | 2 | 2 | 1 | -0.27 | 5.86 | 0.00 |
| 2 | 2 | 2 | 5 | 0.00 | 5.45 | -1.06 |
| 2 | 2 | 2 | 6 | 0.00 | 8.61 | 0.00 |
| 1 | 2 | 2 | 5 | 0.00 | 7.48 | 0.00 |
| 2 | 2 | 6 | 20 | 0.00 | 0.00 | 0.25 |
| 2 | 2 | 6 | 1 | 0.00 | 2.46 | 0.00 |
| 2 | 6 | 1 | 2 | 0.00 | 0.00 | 0.40 |
| 6 | 2 | 2 | 6 | -2.00 | 9.65 | 0.00 |
| 5 | 2 | 2 | 5 | 0.00 | 9.07 | 0.00 |
| 5 | 2 | 2 | 6 | 0.00 | 8.61 | 0.00 |
| 1 | 2 | 2 | 6 | -1.20 | 8.61 | 0.00 |

| Stretch Parameters | | | |
|---|---|---|---|
| Atom Type | | KS | LO |
| 1 | 2 | 4.40 | 1.512 |
| 2 | 2 | 8.08 | 1.392 |
| 2 | 6 | 5.76 | 1.378 |

| Bending Parameters | | | | |
|---|---|---|---|---|
| Atom Type | | | KS | Θ |
| 2 | 2 | 6 | 0.60 | 120.00 |
| 2 | 6 | 20 | 0.35 | 122.00 |
| 2 | 6 | 1 | 0.77 | 113.60 |

Molecular mechanics [Alchemy-II, MMIIPC, MMX and MM2P(87)] and AM1 find the 7-hydroxyl very close to the plane of the A-ring (Table 2). Given the uncertainties in the torsion angles of the hydroxyls from the X-ray structures, the 7-hydroxyl is only marginally different from zero, if at all. The C(13) and C(14) hydroxyl groups of the B-ring are also oriented close to the plane of the aromatic ring in energy minimized structures predicted by all molecular mechanics force fields. The comparatively large displacement of the hydroxyl at C(14) up above the plane of the B-ring in the crystal, again due to hydrogen bonding, is not predicted by these models (Table 2).

Drieding models show interrelated orientations of the C(3) aliphatic hydroxyl and the B-ring. Their coordinated orientation was examined in detail for (-)-epicatechin by Tobiason.[24] To obtain a better global perspective of the energy changes associated with rotational interactions between the B-ring and the C(3)-hydroxyl, the MMX force field was used with the dihedral driver to rotate them through 360° [in 10° and 60° increments for the B-ring and C(3)-OH, respectively]. A three-dimensional plot of energy and torsional angles (Figure 4) was used to analyze various potential energy maxima and minima. In rotation of the B-ring through 360°, two energy maxima occur where the protons on C(12) and C(16) of the B-ring interact with the aliphatic C(3)-OH corresponding to H(2)-C(2)-C(11)-C(12) torsional angles of 20° and 190°. The 20° conformer showed only very slightly higher energy than that at 190° indicating that the placement of similarly aligned hydroxyls on the B-ring had little effect on the energy. A second lower energy interaction of the protons on C(12) and C(16) of the B-ring with the proton on C(3) occurs at H(2)-C(2)-C(11)-C(12) torsional angles of 90° and 270°. A series of six low-energy wells (three orientations of the C(3)-OH at each of two B-ring orientations) was observed. The low-energy B-ring orientations occur at H(2)-C(2)-C(11)-C(12) torsional angles of 150° and 330°. At these B-ring orientations, the C(3)-hydroxyl can be oriented near either 60°, 180° or 300° at minimum energy values that do not differ by more than 0.3 kcal/mol. These differences in energy are so small that MMX does not predict a preferred orientation for the C(3)-hydroxyl. However, AM1 with a H(3)-C(3)-O(2)-H torsion angle of 176° leads to a 2.0 kcal/mol lowering of the structural energy.

The flavan-3-ols and their polymers present especially interesting problems because projected conformations of the pyran rings as determined by measurements of $^3J_{HH}$ coupling constants often do not correspond to either E- or A-conformations. Intermediate coupling constants suggest a dynamic "flipping" between these two conformations on an NMR time scale as first noticed in a study of the penta-acetate of (+)-catechin[17] and more completely defined by Porter and coworkers.[20] The "flipping" molecular dynamics for tetra-*O*-methyl-(+)-catechin have been studied in detail by Mattice et al.[16] For the 2R3S (+)-catechin using the MMX force field, energy barriers for E to A interconversion amounted to 5.4 kcal via a $\beta$-boat and 7.9 kcal via an $\alpha$-boat.[23] Similar computations for 2S3S *ent*-epifisetinidol flipping through an $\alpha$-boat indicate an energy barrier of about 7.2 kcal/mol. Therefore, despite the fact that *ent*-epifisetinidol crystallizes in the E-conformation, dynamic "flipping" between E- and A-conformations must be considered in the solution state. Steynberg,[23] studying (-)-epicatechin, found that E- and A-conformers would be expected to occur in relative proportions of approximately 88:12 (in agreement with Porter[20]) reported by assuming that $^3J_{HH}$ coupling for A and E conformers can be time-averaged to equal the observed coupling constant and hence estimate relative proportions of the two conformers. $^1$H NMR of *ent*-epifisetinidol shows $J_{2,3} = < 2.0$ Hz; $J_{3,4\alpha} = 3.3$ and 16.2 Hz; and $J_{3,4\beta}$ 4.50 and 16.2 Hz, indicating that this compound exists predominantly in the E-conformation in the solution state. In the 2,3-*cis* isomers, the $J_{3,4\beta}$ coupling is most sensitive to the pyran ring conformation. For example, $J_{3,4\beta} = 11.04$ Hz for the MMX optimized A-conformer and only 2.79 Hz for the E-conformer. Using Porter's suggestion that these coupling constants represent a time-averaged mole fraction of A- and E-conformations, the $^1$H-NMR spectra suggest an E:A ratio of about 80:20 for *ent*-epifisetinidol in $d_6$-acetone. An energy difference of +2.09 kcal/mol for the MMX optimized A- over the E-conformer implies an E:A conformer ratio of 98:2 for *ent*-epifisetinidol at 20 °C. This discrepancy in estimates of E:A ratios predicted from $^1$H NMR coupling constants and differences in conformational energy, also observed in other studies, is being addressed in continuing studies.

**Molecular Orbital Analyses of Charge Density Distributions and Reactivity at C(6) and C(8)**

The presence or absence of a C(5) hydroxyl has an enormous influence on the reactivity of the C(6) and C(8) of flavans with electrophiles as well as the stability of the interflavanoid bond.[26] For example, reactions of

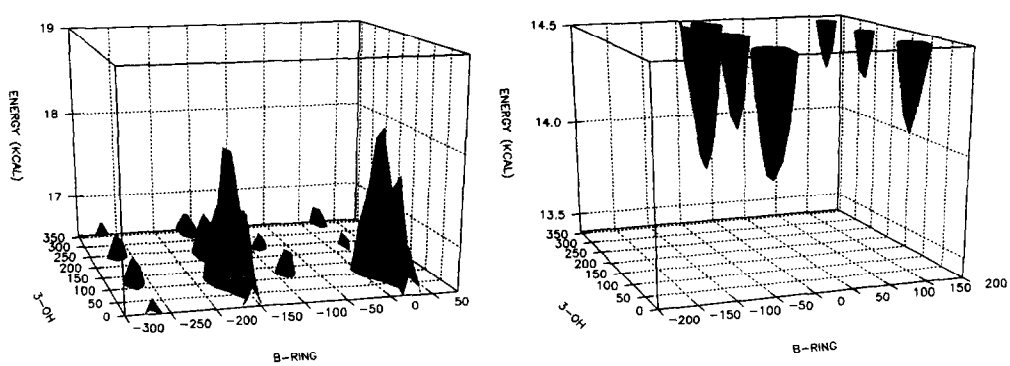


**Figure 4. Interrelated orientations of the aliphatic 3-hydroxyl and B-ring in *ent*-epifisetinidol as estimated by MMX.**

**Table 4.** Regio- and stereo-selectivity in proanthocyanidin synthesis (from Botha et al.[27]).

| Electrophile | Nucleophile | Time (hr) | Linkage | | | |
|---|---|---|---|---|---|---|
| | | | [4α-8] | [4β-8] | [4α-6] | [4β-6] |
| mollisacacidin | fisetinidol | 2 | 0 | 0 | 1.4 | 1 |
| mollisacacidin | fisetinidol | 168 | 0 | 0 | 1.4 | 1 |
| mollisacacidin | *ent*-epifisetinidol | 4.5 | 0 | 0 | 1.3 | 1.0 |
| mollisacacidin | catechin | 12 | 5.1 | 3.0 | 1 | |
| mollisacacidin | catechin | 48 | 12.0 | 9.6 | 1 | 0.2 |
| teracacidin | catechin | 2 | 4.6 | 0 | 1 | -- |
| *ent*-mollisacacidin | catechin | 3 | 10.0 | 13.0 | 1 | -- |
| leucobinetinidin | catechin | 2 | 7.0 | 3.4 | 1 | |
| mollisacacidin | epicatechin | 2 | 30.0 | 24.0 | 1 | |
| leucocyanidin | catechin | 0.5 | 3.2 | 0 | 1 | 0[a] |

[a]Later reports indicate a ratio of 10:1 for [4α→8] and [4α→6] isomers.

(+)-catechin or (-)-epicatechin with *ortho*- or *para*-hydroxybenzyl alcohols result in product ratios of about 2.6:1.0 and 1.2:1.0, respectively.[27] In reactions of (+)-catechin with flavan-carbocations derived from corresponding flavan-3,4-diols, electrophilic substitution is strongly regioselective at C(8).[28,29] However, in procyanidin syntheses catalyzed by acetic acid that are carried out over long time periods (where interflavanoid bonds are continually cleaved and reformed), ratios of C(8):C(6) linked products decrease to an equilibrium of about 1.3:1.0.[30] Measurement of the differences in rate of interflavanoid bond cleavage and equilibrium product ratios of C(8):C(6) linked dimers permitted an approximation of the regioselectivity at C(8):C(6) of about 3.3:1.0

Further examples of the effect of structure on regio- and stereoselectivity of electrophilic substitution of (+)-catechin and (-)-epicatechin are summarized in Table 4 adapted from Botha and coworkers.[28] These results led Roux's school[3] and others[31] to conclude that regioselectivities for the C(8) position in 5,7-hydroxyflavans were due to differences in the bulkiness of the electrophile and the additional steric hindrance at C(6) compared to C(8) due to the pyran ring. Tobiason's[24,32] calculation of partial charge densities at the C(6) and C(8) position of (+)-catechin and (-)-epicatechin using MNDO and AM1 (Figure 5) shows that partial atomic charges are not very different between the C(6) and C(8) positions in agreement with comparisons of their $^{13}C$ NMR chemical shifts (δ 96.8 and 96.0 p.p.m., respectively). In contrast, electrophilic aromatic substitution of the C(5) deoxyflavans (fisetinidol or *ent*-epifisetinidol) is essentially regiospecific at C(6); see Table 4.[28] In profisetinidins terminated with catechin or bi-fisetinidol oligomers, the interflavanoid bond is stable, thus disproportionation does not occur by extending reaction times. Examining the partial charge densities calculated from MNDO and AM1 given for *ent*-epifisetindiol in Figure 5 and noting that the $^{13}C$ NMR chemical shifts for C(6) and C(8) of *ent*-epifisetinidol (δ 109.9 and 104.3 p.p.m., respectively) would suggest from these relative charge densities that a strong preference for reaction at C(6) would not seem likely. Likewise, even though the C(7) hydroxyl is oriented toward C(8) in the crystal and in the MMX

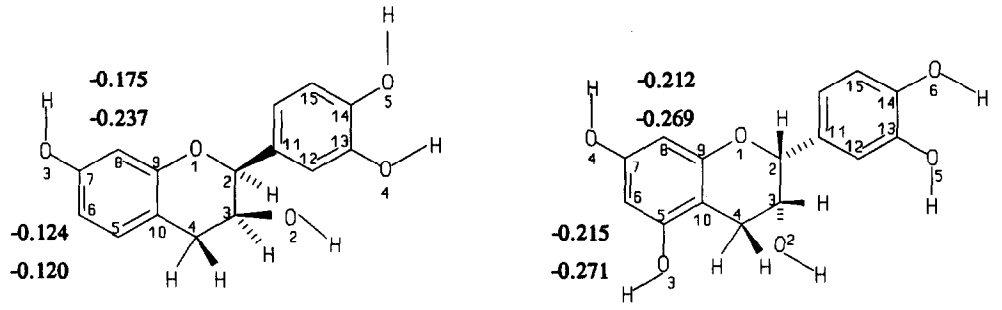


***ent*-epifisetinidol** **(-)-epicatechin**

**Figure 5. Partial atomic charges at C(6) and C(8) found for (-)-epicatechin and *ent*-epifisetinidol using MNDO (upper number) and AM1 (lower number) methods. Distances are in pm and measured from the mean plane of the A-ring.**

calculated low energy conformations, the energy barrier to rotation is comparatively small (about 2.8 kcal/mol), and the energy difference in the two "in plane" conformers was only 0.20 kcal/mol, indicating that the 7-hydroxyl shields the C(6) and C(8) positions equally. Therefore, differences in steric hindrance at the C(6) and C(8) would not seem sufficient to account for a regiospecific reaction at C(6).

In an attempt to resolve this apparent discrepancy, the HOMO charge densities were determined for *ent*-epifisetinidol and are reported in Table 5. The highest occupied molecular orbital (HOMO) is important since it represents the most likely one to take part in a chemical reaction. The coefficients from the frontier molecular orbital[33,34] given both by MNDO and AM1 show that C(6) has a large $P_z$ charge density, whereas, on the C(8) carbon,

**Table 5.** The frontier HOMO and LUMO $P_z$ orbital coefficients for the C(6) and C(8) atoms for *ent*-epifisetinidol using AM1 and MNDO.*

| | MNDO | | AM1 | |
|---|---|---|---|---|
| | HOMO | LUMO | HOMO | LUMO |
| | | E-Conformer | | |
| E, eV | -8.6534 | -0.1645 | -8.8440 | -0.1106 |
| C(6) | 0.5036 | -0.0312 | -0.4572 | -0.0411 |
| C(8) | -0.0080 | 0.0180 | -0.0745 | -0.0304 |
| | | A-Conformer | | |
| E, eV | -8.7937 | -0.1156 | -8.9448 | 0.0128 |
| C(6) | 0.4461 | -0.0629 | 0.4528 | 0.0614 |
| C(8) | -0.0204 | 0.0178 | 0.0314 | -0.0307 |

*The H(3)-C(3)-O(2)-H torsion angle is 168° for the A-conformer with the OH oriented into the pyran ring, and is placed in the higher energy 90° orientation for the E-conformer similar to that in the crystal.

it is near zero. The HOMO coefficient squared is proportional to the charge density at that site. This suggests that even though the partial charge density is large on C(8) it is not favorably oriented for reactivity. Tobiason[24,32] has previously examined total and HOMO charge densities for (-)-epicatechin as estimated by MNDO and AM1 methods. These HOMO frontier MO coefficients are given for (-)-epicatechin in Table 6. The HOMO $\pi$-orbital in *ent*-epifisetinidol is distinct, whereas, in (-)-epicatechin, several upper $\pi$-orbitals are nearly degenerate. Interestingly, the coefficients of the upper near degenerate $\pi$-orbitals are significant and nearly equal in value, suggesting that both C(6) and C(8) have similar propensity toward reactivity, and if steric hindrance or reactant stability is not a factor, would explain why reactions with (-)-epicatechin would possibly equilibrate at nearly 1/1 mixtures between the 6 and 8 positions.

To better understand specific reaction preferences between, for example, (-)-epicatechin and *ent*-epifisetinidol reacting with *para*-hydroxybenzyl alcohol, reaction transition state calculations would need to be accomplished. In this problem, the details of the actual reaction pathway as well as complete evaluation of the HOMO orbital on one reactant and the LUMO orbital on the other and their conformational dependence would be made. This will be reported as part of another study.

In conclusion, this study elucidates the X-ray molecular structure of *ent*-epifisetinidol and shows that PC molecular modeling programs can give considerable success at describing the molecular properties of profisetinidins. In addition, the importance of considering frontier molecular orbitals over using only the total partial electron charge densities in explaining chemical reactivity for *ent*-fisetinidiol has provided an explanation for the unusual regioselectivity in reactions at the C(6) and C(8) of the 5-deoxy profisetinidins.

**Table 6.** The MNDO and AM1 HOMO and LUMO molecular orbital coefficients and respective energies for the E-conformer of (-)-epicatechin.

| | MNDO | | AM1[a] | |
|---|---|---|---|---|
| | HOMO | LUMO | HOMO | LUMO |
| E, eV | -8.8182[b] | -0.0639 | -8.9475 | -0.0220 |
| C(6) | 0.2848 | 0.0592 | -0.2786 | 0.0713 |
| C(8) | 0.2489 | -0.0256 | -0.2671 | -0.0435 |

[a]In the epicatechin A-conformer, the HOMO has both C(6) and C(8) values near zero, but a near-lying orbital in a $\pi_2$ orbital which again shows that both C(6) and C(8) have nearly identical coefficient of 0.270.

[b]A slightly higher energy level at -8.7800 has coefficients for C(6) and C(8) of 0.1942 and 0.0161, respectively, but both neighboring $\pi$ orbitals have large coefficients at C(6) and C(8).

## EXPERIMENTAL

**Compound Isolation and Crystallization:** *Ent*-epifisetinidol, $[\alpha]_D$ = + 76.4° c = 0.235% (acetone-water 1:1 v/v), lit[25] $[\alpha]_D$ = + 82° (acetone-water 1:1 v/v) was isolated from an extract of *Colophospermum mopane* by column chromatography on LH-20 Sephadex with ethanol-water (1:1 v/v) as the eluting solvent. *Ent*-epifisetinidol was eluted slightly ahead of its corresponding 2,3-*trans* isomer. A second separation afforded the chromatographically pure compound that was crystallized from water to give light-brown crystals of the monohydrate.

**Crystal Structure:** The X-ray crystal structure was determined using data collected on an Enraf-Nonius CAD4 diffractometer equipped with $CuK_\alpha$ radiation ($\lambda$=1.54184Å) and a graphite monochromator, by $\omega$-2$\theta$ scans. A full sphere of data was collected within $2<\theta<75°$, and redundant data were averaged to yield 2,708 unique data, of which all but 22 had $I>3\sigma(I)$ and were used in the refinement. Absorption corrections were based on psi scans. The structure was solved by direct methods and refined by full-matrix least squares, including refinement of H atoms, using the VAXSDP[35] set of programs. Convergence was achieved with R=0.03357, $R_w$=0.03843, GOF=2.361. Refinement of the enantiomeric structure under identical conditions yielded R=0.03398, $R_w$=0.03954, GOF=2.430. Thus, the better refinement, illustrated in Figure 1, agrees with the known absolute configuration of [1]. Fractional coordinates are given in Table 1, while bond distances, bond angles, torsion angles, and other derived quantities are given in supplementary material.

**Molecular Modeling:** The modeling packages MMIIPC(77), MM2P(87), and MOPAC 5.0 (AM1 and MNDO) were obtained from the Quantum Exchange Program at the University of Indiana, Bloomington, Indiana. The MOPAC program was run on Digital VAX 6200 machines. The PCs used were 386- and 486-based machines. The Alchemy-II software was obtained from the Tripos Associates, Inc. (St. Louis, Missouri), and MMX was operated from PC-Model 3.3 from Serena Software, Bloomington, Indiana. The MMX program was operated with all aromatic oxygens included in the Pi-system, and the hydrogen bonding function was turned on. The MNDO and AM1 computations were run in the precise mode until a GNORM of 0.5 was reached. The parameters used for MMIIPC were determined from MO-Pi calculations run earlier on MM2P(87) in which the aromatic oxygen atoms were treated as furan type 41 atoms according to Allinger.[36] The remaining type-6 parameters were automatically selected by the program. The only additional change from parameters within MMIIPC was to set the 1 - 2 stretch to 4.400 and 1.512 to better match the crystal structure data obtained from C(2) - C(11) and C(4) - C(10) as shown in Table 3. Work is continuing in an effort to "fine tune" parameters for flavanoids.

Out-of-plain distances were derived from the modeling results by generating the final atomic coordinates using the A-ring as the reference plane. This was accomplished by writing an MNDO file using PC-Model and regenerating an MM file for access to the z-coordinates. The z-coordinates used were corrected for the mean A-ring plane deviation. The preliminary coordinates for the molecules were established from using either Alchemy II or PCMODEL.

## ACKNOWLEDGMENTS

This work was funded in part by USDA Competitive Grants No. 87-FSTY-9-0256 and 91-37103-6492.

## REFERENCES


1. Freudenberg, K.; Fikentscher, H.; Harder, M.; Schmidt, O.; *Justus Liebigs Ann. Chem.* **1925**, 444, 135: Freudenberg, K.; Weinges, K. *Justus Liebigs Ann. Chem.* **1963**, 668, 92.

2. Weinges, K.; Bahr, W.; Ebert, W.; Boritz, K.; Marx, H.-D. *Forschr. Chem. Org. Naturst.* **1969**, 27, 158 and references therein.

3. Roux, D.G.; Ferreira, D. *Fortschr. Chem. Org. Naturst.* **1982**, 41, 48 and references therein; Roux, D.G. *In*: Plant Polyphenols: Synthesis, Properties, Significance, eds. Hemingway, R.W., Laks, P.E., Plenum Press, New York, **1992**, 7.

4. Haslam, E. *In*: The Flavanoids: Advances in Research, ed. Harborne, J.B., Chapman and Hall, London, **1982**, 417: Ya, C.; Gaffney, S.H.; Lilley, T.H.; Haslam, E. *In*: Chemistry and Significance of Condensed Tannins. eds. Hemingway, R.W., Karchesy, J.J. Plenum Press, New York, **1989**, 307.

5. Butler, L.G. *In*: Chemistry and Significance of Condensed Tannins, eds. Hemingway, R.W., Karchesy, J.J., Plenum Press, **1989**, 391.

6. Schultz, J.C. *In*: Chemistry and Significance of Condensed Tannins, eds. Hemingway, R.W.; Karchesy, J.J., Plenum Press, New York, **1989**, 417: Schultz, J.C.; Hunter, M.D.; Appel, H.M. *In*: Plant Polyphenols: Synthesis, Properties, Significance, eds. Hemingway, R.W.; Laks, P.E., Plenum Press, New York, **1992**, 621.

7. Clausen, T.P.; Reichardt, P.B.; Bryant, J.P.; Provenza, F. *In*: Plant Polyphenols: Synthesis, Properties, Significance, eds. Hemingway, R.W.; Laks, P.E. Plenum Press, New York, **1992**, 639.

8. Lees, G.L. *In*: Plant Polyphenols: Synthesis, Properties, Significance, eds. Hemingway, R.W.; Laks, P.E., Plenum Press, New York, **1992**, 915.

9. Slabbert, N. *In*: Plant Polyphenols: Synthesis, Properties, Significance, eds. Hemingway, R.W.; Laks, P.E., Plenum Press, New York, **1992**, 1021.

10. Lea, A.G.H. *In*: Plant Polyphenols: Synthesis, Properties, Significance, eds. Hemingway, R.W.; Laks, P.E. Plenum Press, New York, **1992**, 827.

11. Ottrup, H. *In*: Plant Polyphenols: Synthesis Properties, Significance, eds. Hemingway, R.W.; Laks, P.E., Plenum Press, New York, **1992**, 849.

12. Singleton, V. L. *In*: Plant Polyphenols: Synthesis, Properties, Significance. eds. Hemingway, R.W.; Laks, P.E. Plenum Press, New York, **1992**, 859.

13. McMannus, J.P.; Davis, K.G.; Beart, J.E.; Gaffney. S.H.; Lilley, T.H.; Haslam, E. *J. Chem. Soc. Perkin Trans. II.* **1985**, 1429.

14. Fronczek, F.R.; Gannuch, G.; Mattice, W.L.; Tobiason, F.L.; Broeker, J.L.; Hemingway, R.W. *J. Chem. Soc. Perkin Trans.* II. **1984**, 1611: Spek, A.L.; Kojic-Prodic, B.; Labadie, R.P. *Acta Crystallog.* **1984**, C40, 2069.

15. Porter, L.J.; Wong, R.Y.; Chan, B.G. *J. Chem. Soc. Perkin Trans. I*, **1985**, 1413.

16. Fronczek, F.R.; Hemingway, R.W.; McGraw, G.W.; Steynberg, J.P.; Helfer, C.A.; Mattice, W.L. *Biopolymers*, **1993**, 33, 275.

17. Fronczek, F.R.; Gannuch, G.; Mattice, W.L.; Hemingway, R.W.; Chiari, G.; Tobiason, F.L.; Houglum K.; Shanafelt, H.A. *J. Chem. Soc. Perkin Trans. II.* **1985**, 1383.

18. Engel, D.W.; Hattingh, M.; Hundt, H.K.L.; Roux, D.G. *J. Chem. Soc. Chem. Commun.* **1978**, 695.

19. Boeyens, J.C.A.; Denner, L.; Kolodziej, H.; Roux, D.G. *J. Chem. Soc. Perkin Trans. II.* **1986**, 301.

20. Porter, L.J.; Wong, R.Y.; Benson, M.; Chan, B.G.; Viswanadhan, V.N.; Gandour, R.D.; Mattice, W.L. *J. Chem. Res.* **1986**, (S) 86; (M) 830.

21. Viswanadhan, V.N.; Mattice, W.L. *J. Comput. Chem.* **1986**, 7, 711: Viswanadhan, V.L.; Mattice, W.L. *J. Chem. Soc. Perkin Trans. II.* **1987**, 739.

22. Bergmann, W.R., Barkley, M.D.; Hemingway, R.W.; Mattice, *J. Am. Chem. Soc.* **1987**, 109, 6614: Cho, D.; Tian, R.; Porter, L.J.; Hemingway, R.W.; Mattice *J. Am. Chem. Soc.* **1990**, 112, 4273.

23. Steynberg, J.P.; Brandt, E.V.; Ferreira, D. *J. Chem. Soc. Perkin Trans. II.* **1992**, 1569: Steynberg, J.P.; Brandt, E.V.; Hoffman, M.J.H. Hemingway, R.W.; Ferreira, D. *In*: Plant Polyphenols: Synthesis, Properties, Significance, eds. Hemingway, R.W.; Laks, P.E. Plenum Press, New York, **1992** (in press).

24. Tobiason, F.L. *In*: Plant Polyphenols: Synthesis, Properties, Significance, Plenum Press, eds. Hemingway, R.W.; Laks, P.E, New York, **1992**, 459.

25. Drewes, S.E., Roux, D.G., *J. Chem. Soc. (C)* **1966**, 1644.

26. Hemingway, R.W. *In*: Natural Products in Woody Plants, ed. Rowe, J.W. Springer Verlag, Berlin, **1989**, 571: Hemingway, R.W. *In*: Chemistry and Significance of Condensed Tannins, eds. Hemingway, R.W.; Karchesy, J.J.Plenum Press, **1989**, 249 and references therein.

27. McGraw, G.W.; Hemingway, R.W. *J. Chem. Soc. Perkin Trans. I*, **1982**, 974.

28. Botha, J.J.; Viviers, P.M., Ferreira, D.; Roux, D.G. *J. Chem. Soc. Perkin Trans. I*, **1981**, 1235.

29. Delcour, J.A.; Ferreira, D.; Roux, D.G. *J. Chem. Soc. Perkin Trans. I*, **1983**, 1711.

30. Hemingway, R.W., McGraw, G.W. *J. Wood Chem. Technol.* **1983**, 3, 421.

31. McGraw, G.W. *In*: Chemistry and Significance of Condensed Tannins. eds. Hemingway, R.W.; Karchesy, J.J. Plenum Press, New York, **1989**, 227.

32. Tobiason, F.L.; Hoff, L.A. *In*: Chemistry and Significance of Condensed Tannins, eds. Hemingway, R.W.; Karchesy, J.J. Plenum Press, New York, **1989**, 205.

33. Fleming, I. Frontier Orbitals and Organic Chemical Reactions; Wiley & Sons: New York, **1976**.

34. Fukui, K.; Yonezawa, T.; Shingu, H. *J. Chem. Phys.* **1952**, 20, 722.

35. Frenz, B.A. Enraf-Nonius Structure Determination Package; Enraf-Nonius, Delft, The Netherlands, **1985**.

36. Tai, J.C.; Liu, J.H.; Allinger, N.L. *J. Comput. Chem.* **1987**, 10, 635.